Enzyme conversion of mulberry red pigments in a microfluidic aqueous two-phase system

Xue-Jiao Zhou [1], Wen-Hao Zhao [1], Sheng Sheng [1, 2, 3, 4], Jun Wang [1, 2, 3, 4, *], Fu-An Wu [1, 2, 3, 4, *]

[1] School of Biotechnology, Jiangsu University of Science and Technology, 212018 Zhenjiang, China;
[2] Sericultural Research Institute, Chinese Academy of Agricultural Sciences, 212018 Zhenjiang, China;
[3] Key Laboratory of Silkworm and Mulberry Genetic Improvement, Ministry of Agriculture, Sericultural Research Institute, Zhenjiang 212018, PR China;
[4] Jiangsu Key Laboratory of Sericultural Biology and Biotechnology, Zhenjiang 212018, PR China.
* Corresponding author. *E-mail*: wangjun@just.edu.cn ; fuword@163.com (Prof. Dr. J. Wang & F. A. Wu).

Abstract: The microfluidic aqueous two-phase system can significantly improve the enzyme reaction rate while overcoming the shortcomings of the aqueous phase. It has become one of the important means of biocatalysis and conversion. In the present study, a double Y-branched microfluidic two-phase reactor was successfully prepared. Abandoned mulberry juice was used as substrate. After optimization, 27% ethanol and 18% ammonium sulfate were used as two phases, which were injected into the microchannel at 10 μL/min and 14.5 μL/min, respectively. Based on the immobilized α-L-rhamnosidase catalytic hydrolysis C_3R to C_3G, the reaction was carried out at 45 ℃, pH 5 for 1 h. The conversion of C_3G was 53.78%, which was 34% higher than in conventional reactors. At present, the highest purity of C_3G in the total mulberry red pigments was 64.48%. By HPLC-PDA-ESI-MS, it was successfully obtained high-quality mulberry red pigment. It was proved that the enzyme-catalyzed reaction rate can be greatly improved in this microfluidic aqueous two-phase system. It provides new ideas for microfluidic enzyme catalytic system in waste recovery field.
Keywords: Microfluidic; aqueous two-phase system; immobilized enzyme catalysis; mulberry red pigments.

Introduction

As a natural pigment, mulberry red pigment has been proved to be effective in preventing cancer [1], antioxidation [2] and protecting heart and cerebral vessels [3]. But, due to improper temperature and storage conditions, millions of tons of mulberries are discarded every year. Therefore, it is necessary to recycle the abandoned mulberry. Cyanidin-3-*O*-glucoside (C_3G) is the main component of mulberry red pigments, accounting for about 60% of the total, and cyanidin-3-*O*-rutinoside (C_3R) accounts for about 30% [4]. The difference between C_3G and C_3R is only one rhamnosidic bond. If α-L-rhamnosidase is used to hydrolyze C_3R, the content of C_3G can be close to or even exceed 90%. Finally, a new kind of high-quality mulberry red pigment could be obtained. This will become a hotspot in the field of waste reuse.

In order to increase the content of C_3G in mulberry red pigments, the aqueous two-phase enzyme catalytic technology was used. The aqueous two-phase systems (ATPS) was an incompatible liquid-liquid system consists of inorganic salts and short chain alcohol [5]. The aqueous two-phase enzymatic catalysis system can be simultaneously extracted and catalyzed, which has been widely concerned and applied in the past decades. ATPS has many advantages, such as high extraction rate, mild conditions, low cost, and the potential to achieve the desired product purification and concentration in a single step [6]. In this paper, the use of ATPS enzyme directed catalytic mulberry red pigments can acquire better effect. Furthermore, this can expand the application of ATPS and would have broad market prospects.

However, the aqueous two-phase enzyme catalytic technology has some shortcomings, such as easy emulsification and low separation efficiency [7]. In order to overcome these shortcomings, the microfluidic technology and the aqueous two-phase enzyme catalytic system were combined to obtain the microfluidic aqueous two-phase enzyme catalytic system. Parallel flow is a two-phase flow pattern developed based on the characteristics of fluids that are easily laminar at microscale. Thus, the fluids of each phase are able to maintain their own flow patterns while only reacting with other fluids at the phase-to-phase contact interface [8]. By using parallel flow, the reaction time can be controlled by controlling the length of the microchannel, so that the reaction can be stably carried out and the reaction yield can be improved as much as possible. The degree of diffusion of the interphase particles can be effectively controlled by controlling the flow rate of the fluid, thereby achieving sample mixing, sample reaction and reaction rate control [9]. Meng et al. used urease to catalyze the hydrolysis of urea to produce ammonium carbonate in a double Y-branched microfluidic device. The reaction rate was 500 times higher than that in conventional reactors, and it only took 0.72 seconds [10]. Our previous studies have also demonstrated that enzymatic reactions in microfluidic devices can yield more than 90% of the products [11]. In this paper, a parallel flow microfluidic reactor was used to carry out enzymatic catalysis of mulberry red pigments. Comparing the

catalytic effects of the conventional reactor with the microreactor, in order to obtain the new high quality mulberry red pigment by the best way.

In this study, a double Y-branched aqueous two-phase microfluidic device was designed and manufactured. Ethanol/ammonium sulfate and immobilized enzyme were introduced into the system. The two-phase flow rate, pH, temperature, substrate concentration and other factors were optimized and the reuse times of the immobilized enzyme were studied. Also, the effects of reaction fluids on mass transfer and yield were explored. The kinetics and thermodynamic mechanism were studied. Moreover, the regulation mechanism of microenvironment mass transfer characteristics on enzymatic reaction was revealed, which provided a new method for preparing new high quality mulberry red pigments.

Materials and methods

Design and fabrication of the microfluidic chips

The glass chip of this paper was prepared by standard photolithography, wet chemical etching and room temperature bonding technology [12]. The chip pattern was designed by IllustratorPortable (The width of the Y-channel and the middle straight channel is 300 μm and 600 μm, respectively) and printed into film (Fig. 1a). Firstly, the film was cut into the same as the chrome plate (SG2506, Um, 65 mm*65 mm*1.5 mm, chrome type LRC, chrome thickness 145 nm, glue type S-1805, glue thickness 570 nm, Changsha Shaoguang chrome plate Co., Ltd., Changsha, China) in order to make a photomask. Then the film was covered on the surface of the chrome plate and exposed in a box UV lamp (UVA, 12 W, 365 nm) for 1.5 min. The chrome plate was developed with 0.5% NaOH solution for 2 min. ($Ce(NH_4)_2(N0_3)_6$): CH_3COOH: H_2O=20 g: 3.5 mL: 100 mL) was used to remove the chromium of the chrome plate for 2 min. Afterwards, the plate was solidified at 105 ℃ for 15 min and placed in etching solution (1M HF: NH_4F: HNO_3 = 1:1: 0.5) etched for 150 min at 40 °C. Moreover, it was scrubbed with acetone to remove residual glue. The holes in chrome plate were drilled with a diamond drill bit (0.9*10 mm), after rinsed and dried, the plate was immersed in a Piranha solution (V_{H2O2}: V_{H2SO4} = 1:3) for 30 minutes. Finally, the microfluidic chip was prepared.

The glass chip cover sheet was cut with a glass knife to obtain the same size as the microfluidic chip (SG2506 polished sheet, Um, 65 mm*65 mm*1.5 mm, Changsha Shaoguang Chrome Edition Co., Ltd., Changsha, China). Then, the chips were washed with acetone and pure water. Afterwards, two pieces of chips were bonded in the pure water (ensure no bubbles between two chips). Finally, a stable glass chips were obtained after placed on the heating plate drying for three days at 30 ℃ (Fig. 1b). If there are severe diffraction stripes in chips, they must be re-bonded.

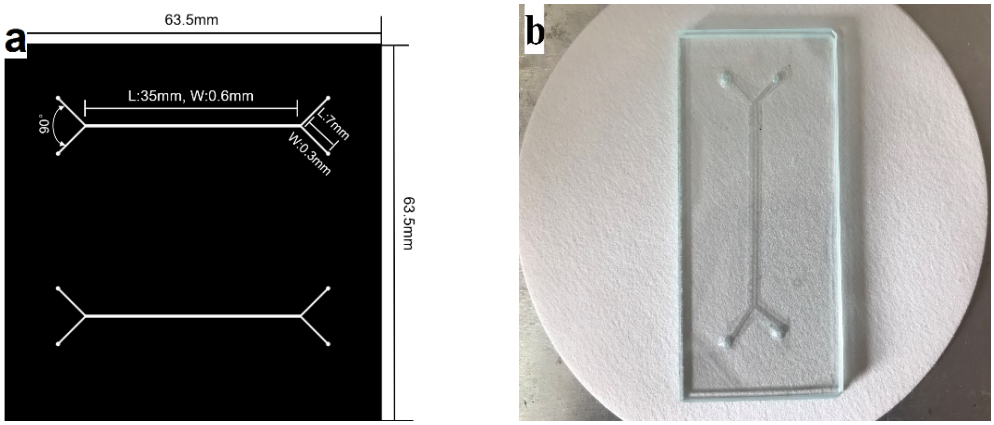

Fig. 1. Design and fabrication of the double Y-branched microfluidic chips. (a) self-designed and printed double Y-branched microchannel film; (b) self-made double Y-branched microchannel chips.

Immobilization of enzyme

The α-L-rhamnosidase was prepared by previous research [13]. During the enzyme immobilization process, Multi-walled carbon nanotube (MWCNTs) was chosen to immobilize α-L-rhamnosidase. 10 mg of MWCNTs was mixed with 2 g of α-L-rhamnosidase crude enzyme solution, and reacted in a water bath at 35 ° C for 8 h. After reaction, the mixture was centrifuged by PBS buffer of pH 7.4 three times at 8000 rpm for 10 min. Discarding the supernatant and the remaining phase was immobilized enzyme. The immobilized enzyme was added into the ammonium sulfate phase to carry out the enzymatic reaction between C_3G and C_3R.

Preparation of aqueous two-phase system

The construction of the aqueous two-phase system was based on the previously reported method [14]. The aqueous two-phase system was composed of 27% (w/w) ethanol, 18% (w/w) ammonium sulfate, 15% (w/w) mulberry juice and the remaining pure water. The entire aqueous two-phase system was placed in a test tube and ultrasonically extracted for 30 min. After equilibrium, the top phase was rich in ethanol and the bottom phase was rich in ammonium sulfate. The ethanol-rich phase with substrate and the ammonium sulfate-rich phase with immobilize *α*-L-rhamnosidase were passed into the reactor from inlet 1 and inlet 2, respectively. The immobilized enzyme and product were collected at outlet 1 and outlet 2, respectively.

Construction of microfluidic aqueous two-phase operating system

The microfluidic chip was fixed on the clamps and the liquid was injected in chip through syringes connected with teflon tubes. The syringes were mainly regulated by constant flow pump (Longer Precision Pump Company, Limited). The ethanol phase with substrate and ammonium sulfate phase with immobilized enzyme were contacted in the middle channel and separated at the end of the Y-branch channel. The teflon tubes at the outlet were used to collect the liquid and detected by HPLC (Fig. 2a).

The phenomenon of aqueous two-phase system in microfluidic chip was showed in Fig. 2b. The top phase was ethanol with substrate, and the bottom phase was ammonium sulfate with immobilized enzyme. By adjusting the two-phase flow rate, the parallel flow two-phase was successfully formed in the microfluidic channel. The flow rate of the top and bottom phase was 11.5 μL/min and 15.5 μL/min, respectively. The Reynolds coefficient of two phases of was 6.75×10^{-4} and 8.79×10^{-4}.

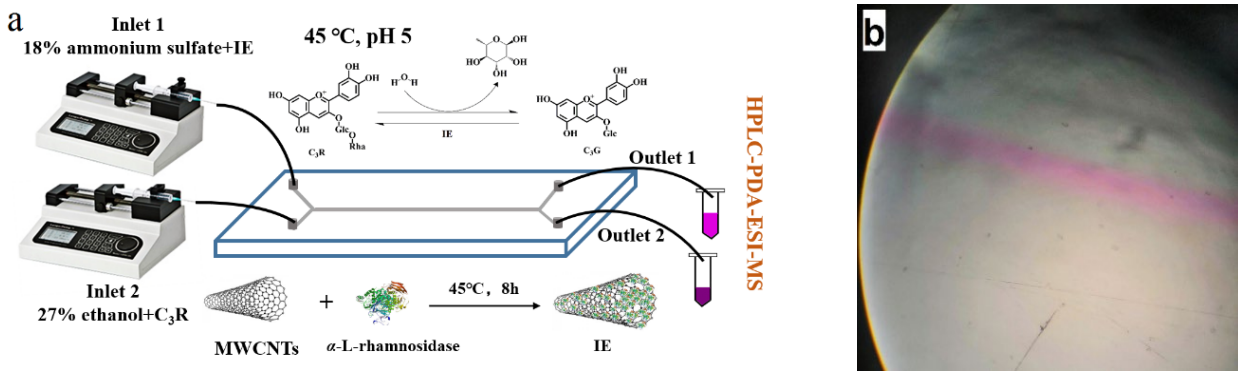

Fig. 2. Construction of microfluidic aqueous two-phase operating system. (a) diagram of microfluidic aqueous two-phase device. (b) photograph of double Y-branched microfluidic channel under the microscope. Reaction conditions: (a) inlet 1 pumped with 18% ammonium sulphate with substrate, inlet 2 pumped with 27% ethanol with immobilized enzyme, correspondingly collected at outlet 1, 2; (b) the top phase was 18% ammonium sulphate with immobilized enzyme., the bottom phase was 27% ethanol with substrate

Enzymatic synthesis of C_3G in microchannel reactor

C_3R hydrolysis of C_3G by immobilized *α*-L-rhamnosidase was carried out in the prepared microchannel reactor. The effects of ammonium sulfate flow rate (13.5-18 μL/min), ethanol flow rate (8-12.5 μL/min), pH (3.5-5), temperature (30-50 °C) and conclentration of mulberry juice (0.02-0.24 mg/mL) in the microchannel on the conversion rate were investigated. After reaction, the content of C_3G and the C_3R was detected by HPLC. The samples before and after the reaction were lyophilized and weighed to be tested. All the experiments were carried out in triplicate.

V was the volume of the microchannel. It was calculated using the following equations:

$$V = L \times W \times d \tag{1}$$

L is the length of the microchannel, *W* is the width of the microchannel, *d* is the deep of the microchannel. τ was the residence time of the fluid in the microchannel. It was calculated using the following equations:

$$\tau = \frac{\frac{1}{2}V}{Q} \tag{2}$$

V is the volume of the microchannel, *Q* is the flow rate of fluid in the microchannel. The conversion (*Y*) was the ratio of C_3G in the microchannel reactor. It was calculated using the following equations:

$$Y(\%) = \frac{\frac{C_{C_3G}}{484}}{\frac{C_{C_3R}}{630}} \times 100\% \quad (3)$$

C_{C3G} and C_{C3R} is the concentration of the substrate and product respectively. C was the content of C_3G in the total mulberry red pigments. It was calculated using the following equations:

$$C(\%) = \frac{m_{C_3G}}{m_{总}} \times 100\%$$

Characterization analysis

FT-IR spectra studied the prepared samples of immobilized enzyme, which were recorded on a BRUKER TENSOR [15]. Scanning Electron Microscope SEM (HITACHI S-4700) observed microstructures and surface morphologies of enzyme, immobilized materials and polymers with immobilized enzyme, respectively.

Analysis of C_3G and C_3R by HPLC–PDA-ESI-MS

The steps of mulberry red pigment sample preparation were as follows [16]: fresh mulberries were collected on the farm of Sericultural Research Institute (Jiangsu University of Science and Technology, Zhenjiang, Jiangsu, China). Juice was extracted on the day after picking, filtered, centrifuged at 8000 rpm/min and stored at 4 °C. 100 mg of lyophilized mulberry powder was added to 1 mL of extractant (methanol: water: 0.1% formic acid = 70:30:1, v/v/v), The mixture was vortexed for 1 hour and sonicated for 20 min.

The HPLC-ESI-MS/MS analytical method of mulberry red pigment was based on previous research [17]. The HPLC-ESI-MS/MS system used in this study were performed by Waters 2695 with Waters 2998PDA and TSQ series mass spectrometer system. Thermo C_{18} (50× 2.1 mm, 5 μm) was used to separate and determinate C_3G and C_3R. The column was maintained at 35 °C and the injection volume was 2 μL. All solutions were filtered through a 0.45 μm filter before injection. The mobile phase consisted of 0.1% formic acid (solvent A) and 100% methanol (solvent B) at a flow rate of 0.4 mL/min. The gradient elution scheme was as follows: 0-5min, 10%B; 5-30min, 30%B; 30-35min, 88%B; 35-45min, 10%B. C_3G and C_3R were detected at 513 nm. The conditions of ESI-MS were as follows: positive mode, spray voltage 3500V, vaporizer temperature 350 ° C, sheath gas pressure 70 psi, aux gas pressure 20 psi, capillary temperature 350 ° C, tube lens offset 62 and scan range 100–1000 m/z.

Reusability tests of immobilized enzyme

Reusability tests for immobilized enzymes were performed under optimal experimental conditions as follows [18]: in microchannel reactor, the flow rate of ethanol was 10 μL/min, the flow rate of ammonium sulfate was 14.5 μL/min. Two kinds of fluids inlet into microchannel at pH 5, 45 °C for 30min. After each reaction, the immobilized enzyme was centrifuged for 10 min at 8000 rpm and carefully washed with PBS for three times in order to remove residual mixture. Finally, a fresh immobilized enzyme was added into a new microfluidic aqueous two-phase system.

Statistical analysis

All experiments were performed in triplicate. The final values were expressed as mean ± standard deviation. One-way analysis of variance (ANOVA) was performed to analyze the variance of these results, and the use of Origin Pro 8.0 was significant at $P < 0.05$.

Results and discussion

Analysis of immobilized enzyme

In this study, MWCNTs was used as immobilized material to immobilize α-L-rhamnosidase. Fig. 3a shows the image of the crude enzyme solution before immobilization. Fig. 3b and Fig. 3c shows the difference on the surface micromorphology of MWCNTs before and after immobilization. It was observed that a small amount of enzyme was adhered to MWCNTs. It can be preliminarily determined that the enzyme had been fixed on MWCNTs. SEM is an important tool for studying surface morphology and internal microstructure, which revealed the excellent performance of MWCNTs used as supporter for α-L-rhamnosidase immobilization.

Fig. 4 depicts the FT-IR spectra of α-L-rhamosidase, MWCNTs and MWCNTs immobilized enzyme. The emission spectrum of α-L-rhamosidase showed peaks at 3289 cm^{-1}, 1653 cm^{-1}, 1541 cm^{-1}, 1455 cm^{-1}, 1399 cm^{-1},

1237 cm^{-1}, 1079 cm^{-1}, which corresponds to ν(O–H)/ν(N–H), C=O bond, amide II, ν(COO–)/ν(C=C), amide III, amide III, δ(N-H) vibration modes, respectively [19]. The infrared absorption peaks of MWCNTs immobilized enzyme were basically consistent with the peaks of *α*-L-rhamosidase. It is owing to the spectra of MWCNTs was very weak and almost absent [20], which due to the high purity of the MWCNTs and its physical properties. Overall, these characteristic peaks further confirmed that *α*-L-rhamnosidase was successfully immobilized on MWCNTs.

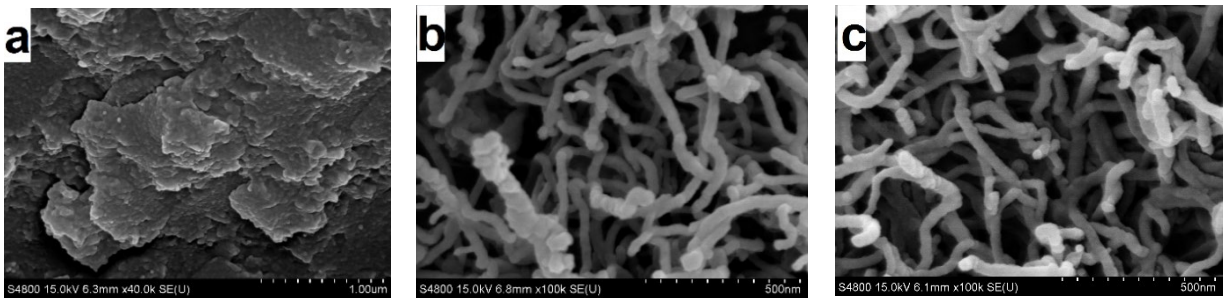

Fig. 3. The SEM photos of *α*-L-rhamosidase before (a) and after (c) immobilization on the immobilization materials(b). Reaction conditions: The crude enzyme solution (2 mL) was added to the immobilized material (10 mg), and reacted in water bath shaker for 8 hours at the temperature of 45 °C.

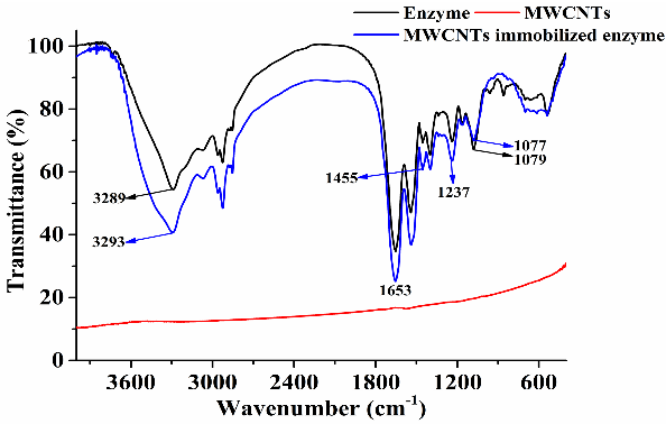

Fig. 4. The FT-IR spectra of *α*-L-rhamosidase, MWCNTs and MWCNTs immobilized enzyme. Reaction conditions: The crude enzyme solution (2 mL) was added to the immobilized material (10 mg), and reacted in water bath shaker for 8 hours at the temperature of 45 °C.

Effect of ammonium sulfate flow rate on C_3G conversion rate

Through experiments, when the ammonium sulfate flow rate was in the range of 13.5-18 *μ*L/min, a stable parallel flow two-phase system could be formed in the microchannel. Fig. 5a shows the influence of ammonium sulfate flow rate on the conversion of C_3G. The conversion of C_3G was increased first and then decreased. When the rate of ammonium sulfate increased to 14.5 *μ*L/min, the conversion of C_3G reached the maximum value of 39.98%. Correspondingly, C_3G the highest purity of in the total mulberry red pigments, which was 60.29%. When ammonium sulfate flow rate continued to increase, the conversion rate of C_3G began to decrease. The fundamental reason was that since the length of the microfluidic channel was constant, with the increase of ammonium sulfate flow rate, the contact time (τ) of the two phases decreased. That is, the reaction time was decreased. As observed in Table 1, when the flow rate of ethanol phase was fixed at 11 *μ*L/min, as the flow rate of ammonium sulfate phase increased from 13.5 *μ*L/min to 18 *μ*L/min, τ was decreased from 10.5 s to 7.88 s. Undoubtedly, within a certain range, the longer the residence time of the fluid, the longer the contact time between enzyme and substrate, and the higher the conversion rate of C_3G was. However, when the flow rate of ammonium sulfate was increased, on the one hand, the contact time between the enzyme and the substrate was reduced, leading to incomplete reaction [21]. On the other hand, it may lead to increased friction between the fluid and the inner wall of the microchannel, resulting in increased shear force and local temperature, which may lead to reduction of enzyme activity, and ultimately reduce the conversion rate of C_3G [22]. when the ammonium sulfate flow rate was 14.5, Therefore, 14.5 *μ*L/min was selected as a suitable flow rate of ammonium sulfate for subsequent research.

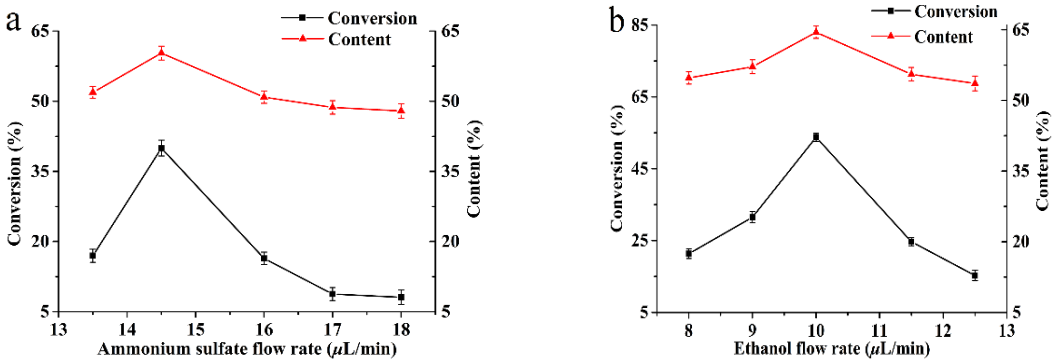

Fig. 5. Effect of flow rate on C_3G conversion rate. (a) effect of ammonium sulfate flow rate on C_3G conversion rate; (b) effect of ethanol flow rate on C_3G conversion rate. Reaction conditions: (a) concentration of mulberry juice was 0.08 mg/mL, temperature was 30 °C, pH was 4.5, the ethanol flow rate was 11μL/min, the ammonium sulfate flow rate was ranged from 13.5-18 μL/min; (b) concentration of mulberry juice was 0.08 mg/mL, temperature was 30 °C, pH was 4.5, the ammonium sulfate flow rate was 14.5 μL/min, the ethanol flow rate was 8 - 12.5 μL/min.

Table 1 Residence time of fluid in microchannels at different flow rates. The ethanol flow rate was 11μL/min, the residence time of the fluid in the channel when changing the ammonium sulfate flow rate.

Ethanol flow rate (μL/min)	Ammonium sulfate flow rate (μL/min)	Residence time τ (s)
11.00	13.50	10.50
11.00	14.00	10.12
11.00	14.50	9.77
11.00	16.00	8.86
11.00	16.50	8.59
11.00	17.00	8.33
11.00	17.50	8.10
11.00	18.00	7.88

Effect of ethanol flow rate on C_3G conversion rate

The ammonium sulfate flow rate was set to 14.5μL/min. When the ethanol flow rate was in the range of 8-12.5 μL/min, a stable aqueous two-phase system could be formed in the microchannel. Fig. 5b shows the influence of ethanol flow rate on the conversion of C_3G. The conversion of C_3G was also increased first and then decreased. When the rate of ethanol increased to 10 μL/min, the conversion of C_3G reached the maximum value of 53.78%. Correspondingly, C_3G the highest purity of in the total mulberry red pigments, which was 64.48%. The same as the effect of ammonium sulfate flow rate, the residence time had a great influence on the conversion of C_3G with the change of ethanol flow rate. As is shown in Table 2, as the flow rate of ethanol increased from 8 μL/min to 12.5 μL/min, τ was decreased from 17.72 s to 11.34 s. The short residence time limited the conversion rate of enzymatic reaction. More importantly, ethanol has a certain inhibitory effect on enzyme activity. Ethanol could absorb the water molecules bound to the non-polar groups of proteins, so that these groups would be exposed and attract or repel each other, resulting in the change of protein spatial conformation and the deactivation of enzymes [23].

Table 2 Residence time of fluid in microchannels at different flow rates. The ammonium sulfate flow rate was 14.5μL/min, the residence time of the fluid in the channel when changing the ethanol flow rate.

Ethanol flow rate (μL/min)	Ammonium sulfate flow rate (μL/min)	Residence time τ (s)
8.00	14.50	10.50
8.50	14.50	10.12
9.00	14.50	9.77
9.50	14.50	8.86
10.00	14.50	8.59
11.00	14.50	8.33
11.50	14.50	8.10
12.00	14.50	7.88
12.50	14.50	14.5

Therefore, the use of MWCNTs to immobilize α-L-rhamnosidase could protect the enzyme from ethanol inhibition to some extent [24]. But when the flow rate of ethanol was too high, this protection did not work very well. Overall, 10 μL/min was selected as the optimum flow rate of ethanol for further studies.

Identification of mulberry red pigments by HPLC-PDA-ESI-MS

After pretreatment, the reaction samples were analyzed by HPLC-PDA-ESI-MS. Fig. 6a shows the HPLC chromatogram of mulberry red pigments. After gradient elution, two peaks were separated. The retention times (Rt) of these two peaks were 8.40 min and 10.21 min respectively. Fig. 6b shows the total ion chromatogram and mass spectrum of peak 1. Peak 1 (Rt =8.64 min), showed $[M]^+$ at *m/z* 449, which was considered to be C_3G. Fig. 6c shows the total ion chromatogram and mass spectrum of peak 2. Peak 2 (Rt =10.41 min), showed $[M]^+$ at *m/z* 595 which was considered to be C_3R [25]. Finally, it was successfully determined that there were two kinds of anthocyanins in mulberry red pigments, C_3G and C_3R.

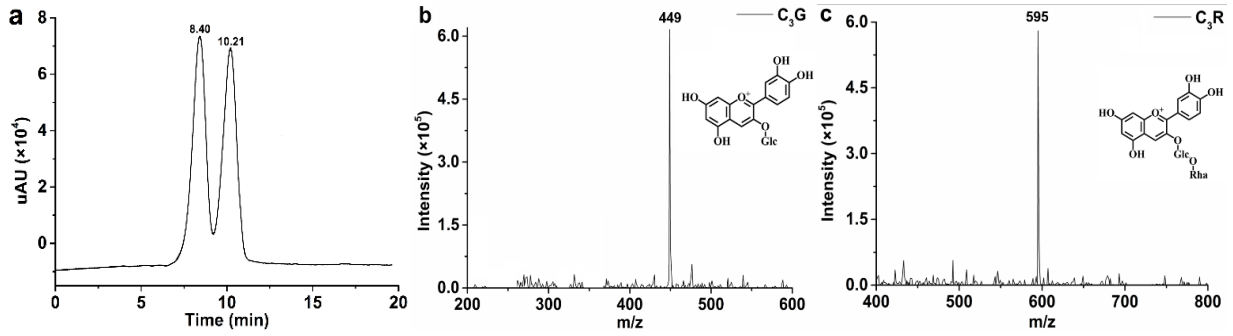

Fig. 6. HPLC–PDA-MS/MS chromatograms of the product in microfluidic aqueous two-phase enzyme catalytic system. (a) the HPLC chromatograms of the mulberry red pigments; (b) the ESI full mass chromatogram of C_3G; (c) the ESI full mass chromatogram of C_3R.

Conclusions

A microfluidic aqueous two-phase enzyme catalytic system was successfully constructed. Firstly, a dual Y-branched glass chip was prepared as a microchannel reactor using standard photolithography, wet chemical etching and room temperature bonding techniques. After optimization, 27% ethanol and 18% ammonium sulfate were used as two phases, which were injected into the microchannel at 10 μL/min and 14.5 μL/min, respectively. Based on the immobilized α-L-rhamnosidase catalytic hydrolysis C_3R to C_3G, the reaction was carried out at 45 ℃, pH 5 for 1 h. The conversion of C_3G was 53.78%, which was 34% higher than in conventional reactors. At present, the highest purity of C_3G in the total mulberry red pigments was 64.48%. By HPLC-PDA-ESI-MS, it was successfully obtained high-quality mulberry red pigments, which provides a new method for microfluidic biosynthesis of waste reuse.

Acknowledgments

This work was supported by the Natural Science Foundation of China (21676130), the Key Project of University Science Research of Jiangsu Province (16KJA530002), the Qing Lan Project of Jiangsu Province (Year of 2014), the Six Talent Peaks Project of Jiangsu Province (2015-NY-018), and the Shen Lan Young scholars program of Jiangsu University of Science and Technology (Year of 2015).

The authors have declared no conflicts of interest.

Reference:

1. Castañeda, A., Pacheco, H.L., Páez, E., Rodriguez, J., Galán-Vidal, C. Chemical studies of anthocyanins: A review. Food Chemistry, **113**(4), 859-871 (2009).
2. Sheng, F., Wang, Y.N., Zhao, X.C., Tian, N., Hu, H.L., Li, P.X. Separation and identification of anthocyanin extracted from mulberry fruit and the pigment binding properties toward human serum albumin. Journal of Agricultural and Food Chemistry, **62**(28), 6813-6819 (2014).
3. Khalifa, I., Zhu, W., Li, K.K., Li, C.M. Polyphenols of mulberry fruits as multifaceted compounds: Compositions, metabolism, health benefits, and stability-A structural review. Journal of Functional Foods, **40**(1), 28-43 (2018).
4. Natic, M.M., Dabic, D.C., Papetti, A., Aksic, M.M.F., Ognjanov, V., Ljubojevic, M., Tesic, Z.L. Analysis and characterisation of phytochemicals in mulberry (*Morus alba L.*) fruits grown in Vojvodina, North Serbia. Food Chemistry, **171**, 128-136 (2015).

5. Qin, B.L., Liu, X.C., Cui, H.M., Ma, Y., Wang, Z.M., Han, J. Aqueous two-phase assisted by ultrasound for the extraction of anthocyanins from *Lycium ruthenicum Murr*. Preparative Biochemistry & Biotechnology, **47**(9), 881-888 (2017).
6. Loureiro, D.B., Braia, M., Romanini, D., Tubio, G. Partitioning of xylanase from thermomyces lanuginosus in PEG/NaCit aqueous two-phase systems: Structural and functional approach. Protein Expression and Purification, **129**, 25-30 (2017).
7. Li, S., Cao, X. Enzymatic synthesis of cephalexin in recyclable aqueous two-phase systems composed by two pH responsive polymers. Biochemical Engineering Journal, **90**, 301-306 (2014).
8. Novak, U., Lakner, M., Plazl, I., Žnidaršič-Plazl, P. Experimental studies and modeling of α-amylase aqueous two-phase extraction within a microfluidic device. Microfluidics and Nanofluidics, **19**(1),75-83 (2015).
9. SooHoo, J.R., Walker, G.M. Microfluidic aqueous two-phase system for leukocyte concentration from whole blood. Biomedical Microdevices, **11**(2), 323-329 (2009).
10. Meng, S.X., Xue, L.H., Xie, C.Y. Enhanced enzymatic reaction by aqueous two-phase systems using parallel-laminar flow in a double Y-branched microfluidic device. Chemical Engineering Journal, **335**, 392-400 (2018).
11. Gong, A., Zhu, C.T., Xu, Y., Wang, F.Q., Tsabing, D.K., Wu, F.A., Wang, J. Moving and unsinkable graphene sheets immobilized enzyme for microfluidic biocatalysis. Scientific Reports, **7**(1), 4309-4323 (2017).
12. Mehboudi, A., Yeom, J. A two-step sealing-and-reinforcement SU8 bonding paradigm for the fabrication of shallow microchannels. Journal of Micromechanics and Microengineering, **28**(3), 035002 (2017).
13. Wang, F., He, S., Zhu, C., Rabausch, U., Streit, W., Wang, J. The combined use of a continuous-flow microchannel reactor and ionic liquid cosolvent for efficient biocatalysis of unpurified recombinant enzyme. Journal of Chemical Technology & Biotechnology, **93**(9), 2671-2680 (2018).
14. Wu, X., Liang, L., Zou, Y., Zhao, T., Zhao, J., Li, F., Yang, L. Aqueous two-phase extraction, identification and antioxidant activity of anthocyanins from mulberry (*Morus atropurpurea Roxb*.). Food Chemistry, **129**(2), 443-453 (2011).
15. Juang, R.S., Tseng, R.L., Wu, F.C., Lee, S.H. Adsorption behavior of reactive dyes from aqueous solution on chitosan. Journal of Chemical Technology and Biotechnology, **70**(4), 391-399 (1997).
16. Barnes, J., Nguyen, H., Shen, S., A Schug, K. General method for extraction of blueberry anthocyanins and identification using high performance liquid chromatography-electrospray ionization-ion trap-time of flight-mass spectrometry. Journal of Chromatography. A, **1216**(23), 4728-4735 (2009).
17. Fan, H.J., Wrolstad, R. Anthocyanin pigment composition of blackberries. Journal of Food Science, **70**(3), 198-202 (2006)
18. Meller, K., Szumski, M., Buszewski, B. Microfluidic reactors with immobilized enzymes-Characterization, dividing, perspectives. Sensors and Actuators B: Chemical, **244**, 84-106 (2017).
19. Antón-Millán, N., García-Tojal, J., Marty Roda, M., Garroni, S., Cuesta-Lopez, S., Tamayo-Ramos, J.A. Influence of three commercial graphene derivatives on the catalytic properties of a *Lactobacillus* plantarum α-L-rhamnosidase when used as immobilization matrices. ACS Applied Materials & Interfaces, **10**(21), 18170-18182 (2018).
20. Rastian, Z., Khodadadi, A.A., Vahabzadeh, F., Bortolini, C., Dong, M., Mortazavi, Y., Mogharei, A., Vesali-Naseh, M., Guo, Z. Facile surface functionalization of multiwalled carbon nanotubes by soft dielectric barrier discharge plasma: Generate compatible interface for lipase immobilization. Biochemical Engineering Journal, **90**, 16-26 (2014).
21. Silva, D., Azevedo, A., Fernandes, P., Chu, V., Conde, J.P., Aires-Barros, M. Design of a microfluidic platform for monoclonal antibody extraction using an aqueous two-phase system. Journal of chromatography. A, **1249**, 1-7 (2012).
22. Al-Shamani, A., Sopian, K., Mohammed, H., Sohif, M., Ruslan, M.H., Abed, A. Enhancement heat transfer characteristics in the channel with trapezoidal rib-groove using nanofluids. Case Studies in Thermal Engineering, **35**(5), 48-58 (2014).
23. Nikolaidis, A., Moschakis, T. On the reversibility of ethanol-induced whey protein denaturation. Food Hydrocolloids, **84**, 389-395 (2018).
24. Khan, M., Husain, Q., Bushra, R. Immobilization of β-galactosidase on surface modified cobalt/multiwalled carbon nanotube nanocomposite improves enzyme stability and resistance to inhibitor. International Journal of Biological Macromolecules, **105**(1), 226-237 (2017).
25. Diaconeasa, Z., Ayvaz, H., Rugină, D., Leopold, L., Stanila, A., Socaciu, C., Tabaran, F., Luput, L., Mada, D., Pintea, A., Jefferson, A. Melanoma inhibition by anthocyanins is associated with the reduction of oxidative stress biomarkers and changes in mitochondrial membrane potential. Plant Foods for Human Nutrition, **72**(4), 404-410 (2017).